

Research Article

Applying a Nonspin-Flip Reaction Scheme to Explain for the Doublet Sulfide Oxides SMO_2 Observed for the Reactions of SO_2 with $\text{V}(^4\text{F})$, $\text{Nb}(^6\text{D})$, and $\text{Ta}(^4\text{F})$

Carlos Velásquez,¹ Ana E. Torres,² Jorge M. Seminario ² and Fernando Colmenares ¹

¹Departamento de Física y Química Teórica, Facultad de Química, Universidad Nacional Autónoma de México, CDMX 04510, Mexico

²Department of Chemical Engineering, Texas A&M University, College Station, TX 77843, USA

Correspondence should be addressed to Jorge M. Seminario; seminario@tamu.edu and Fernando Colmenares; colmen@unam.mx

Received 17 January 2018; Accepted 5 March 2018; Published 1 April 2018

Academic Editor: Carlos R. Cabrera

Copyright © 2018 Carlos Velásquez et al. This is an open access article distributed under the Creative Commons Attribution License, which permits unrestricted use, distribution, and reproduction in any medium, provided the original work is properly cited.

Energy profiles linking the reactants $\text{M} + \text{SO}_2$ ($\text{M} = \text{V}(^4\text{F})$, $\text{Nb}(^6\text{D}; ^4\text{F})$, and $\text{Ta}(^4\text{F})$) with the products observed for these reactions under matrix-isolation conditions, mainly the oxide complex $\text{OV}(\eta_2\text{-SO})$ and the sulfide oxides SVO_2 , SNbO_2 , and STaO_2 , have been obtained from DFT and CASSCF-MRMP2 calculations. For each of these interactions, the radical fragments $\text{MO} + \text{SO}$ can be reached from the lowest-lying quadruplet electronic states of the reactants. As the quadruplet and doublet radical asymptotes that vary only in the spin of the unpaired parallel electrons of the nonmetallic fragment are degenerated, a second reaction leading to the rebounding of the radical fragments can take place through both multiplicity channels. Reaction along the doublet pathway leads in each case to the most stable structure for the oxide SMO_2 . For the vanadium interaction, recombination of the radical species through the quadruplet channel explains for the oxide product $\text{OV}(\eta_2\text{-SO})$.

1. Introduction

Besides being an uncontrollable air contaminant, sulfur dioxide is also a poison in many catalytic processes [1–3]. The study of the activation of the S-O bond by transition metal containing systems has been one of main lines followed to explore the factors that could favor the decomposition of this molecule. Most of these studies have been focused in analyzing the adsorption and decomposition processes of SO_2 in pure metals, alloys, and metal oxides [4–9]. Kinetic investigations have also been carried out on the reactions of this molecule with different transition metal atoms. Results emerging from those studies show that SO_2 is more reactive than other gases (O_2 , SO_2 , CO_2 , N_2 , N_2O , and NO) in this kind of reactions [10–14].

The interaction of SO_2 with laser-ablated transition metal atoms in groups IV–VI of the periodic table has been investigated by IR spectroscopy under matrix-isolation

conditions [15–17]. The main products observed for these interactions are the oxide complex $\text{OM}(\eta_2\text{-SO})$ and/or the sulfide oxide SMO_2 . Importantly, for most of these reactions, the spin multiplicity assigned to the products does not match the spin corresponding to the ground state of the reactants. For example, the frequencies detected in the IR-matrix spectra for the products emerging from the reactions $\text{M} + \text{SO}_2$ ($\text{M} = \text{V}(^4\text{F})$, $\text{Nb}(^6\text{D})$, and $\text{Ta}(^4\text{F})$), mainly the complex $\text{OV}(\eta_2\text{-SO})$ and the sulfide oxides SMO_2 ($\text{M} = \text{V}$, Nb , Ta), fit better those determined through DFT calculations for the corresponding doublet structures [17]. Liu et al. rationalized the different spin multiplicity between the reactants and the products by invoking interactions between electronic states of different spin through intersystem-crossings. For instance, they proposed that the vanadium reaction undergoes through an intersystem crossing between the potential energy curves emerging from the quadruplet ground state and the first excited doublet state of the reactants. In our opinion,

the use of spin-flip models could be inadequate for the theoretical description of reactions in which only rather light elements participate. For these reactions, it is not expected that the relativistic effects that lead to interactions of electronic states of different spin be relevant. In addition, doublet electronic states do not appear among the low-lying states for the vanadium atom, so it is unlikely that they take place in reactions proceeding under cryogenic conditions [18].

Recently, we studied theoretically the interactions of acetonitrile with group V transition metal atoms [19]. In accord with the results in reference 19, the products determined under matrix-isolation conditions for these reactions can be explained in terms of a nonspin flip scheme consisting of two sequential reactions involving the radical species $M\text{-NC} + \text{CH}_3$. For the niobium and tantalum reactions, these radical fragments are energetically accessible; thus, they could be reached from the ground state of the reactants. As the radical moieties remain caged at the matrix, they can recombine themselves in a second reaction to yield the inserted structure $\text{CH}_3\text{-M-NC}$. Like the quadruplet and doublet asymptotes $M\text{-NC} + \text{CH}_3$ that vary only in the spin of the methyl group are degenerate, the rebounding reaction can take place along both multiplicity channels. Once the inserted structure $\text{CH}_3\text{-M-NC}$ has been formed, the low-multiplicity channel leads to the products detected for these interactions by migration of one or two hydrogen atoms toward the metal atom. According to this scheme, the lack of inserted structures in the product distribution determined for the vanadium reaction could be rationalized in terms of the high energy found for the radical species $V\text{-NC} + \text{CH}_3$.

In this contribution, we use a similar two-step reaction scheme to describe the interactions of the SO_2 molecule with the same group of transition metal atoms. It is shown that the results obtained for each of the investigated reactions allow to rationalize the product distributions observed for them in the IR-matrix spectra, without invoking interactions between electronic states of different spin multiplicity.

2. Computational Details

For all the investigated reactions, DFT-B3LYP-Def2-TZVP and CASSCF-MRMP2 calculations were performed to obtain the energy profiles that join the ground state of the reactants with the observed products in the IR-matrix spectra, mainly the oxide complex $\text{OM}(\eta_2\text{-SO})$ and the sulfide oxide SMO_2 . Since the lowest-lying excited quadruplet state of niobium lies only 3.5 kcal/mol above the sextuplet ground state, the energy profile emerging from the fragments $\text{Nb}({}^4\text{F}) + \text{SO}_2$ was also calculated [18]. All the located stationary points were characterized as energy minima or transition states through frequency analysis calculations at DFT level of theory. These calculations were done employing the functional B3LYP as used before by Liu et al. in a previous contribution on the investigated interactions for comparing the theoretical frequencies with the experimental ones [17]. Inclusion of a portion of exact exchange from Hartree-Fock theory using a hybrid functional can be important for the comparative description of systems involving electronic states with unpaired electrons, such as the quadruplet and doublets

electronic states studied in this contribution. The energy of each of the stationary points was reevaluated through single-point CASSCF-MRMP2 calculations.

For each of the investigated interactions, the energies of the lowest-lying quadruplet and doublet radical fragments $\text{MO} + \text{SO}$ that vary only in the spin of the unpaired parallel electrons of the SO fragment were calculated at CASSCF-MRMP2 level of theory. Likewise, potential energy curves for the rebounding of the radical fragments to yield the metal oxide structure $\text{OM}(\eta_2\text{-SO})$ were obtained from partial geometry calculations by approaching perpendicularly the metal fragment to the SO radical at different distances, without any additional symmetry restrictions.

For all the atoms, the Def2-TZVP basis sets optimized by Weigend and Ahlrichs were used [20–22]. The niobium and tantalum atoms were described using the pseudopotentials proposed by Dolg et al., which include 28 and 60 electrons in the inner core, respectively [23].

The CASSCF calculations were carried out using an active space consisting of 7 electrons in 7 active orbitals, which expands around 700 CSF's. The orbital space included in all the cases the d- and s-type functions of the transition metal atom as well as the outermost p-type functions of sulfur and oxygen. MRMP2 calculations were carried out using the same active space.

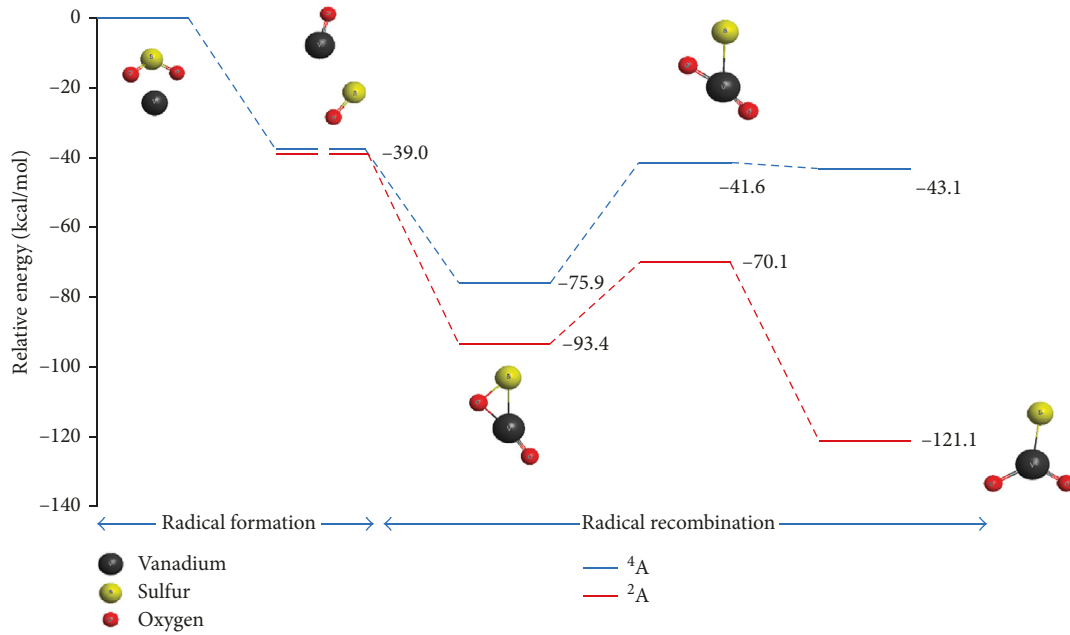
All the calculations were performed using the GAMESS and GAUSSIAN09 computational packages [24, 25].

3. Results and Discussion

3.1. $V + \text{SO}_2$ Reaction. In Figure 1 are shown the two sequential radical reactions that lead from the ground state of the reactants $V({}^4\text{F}) + \text{SO}_2$ to the products observed for this interaction under matrix-isolation conditions, mainly the oxide $\text{OV}(\eta_2\text{-SO})$ and the sulfide oxide SVO_2 compounds [17]. Geometrical parameters for these structures are provided in Table 1.

As it is seen in Figure 1, the radical fragments $\text{VO} + \text{SO}$ lie 39 kcal/mol below the ground state reference. Hence, it is plausible that these radical species are yielded from the reactants $V({}^4\text{F}) + \text{SO}_2$ in a first reaction. It has been proposed that a rhombic intermediate arising from the electrostatic interaction between the fragments could be formed in the first stage of the reaction [17].

However, the potential well calculated for this structure is only 1.7 kcal/mol below the energy corresponding to the radical species $\text{VO} + \text{SO}$. Hence, it could be expected that the reaction taking place from the ground state of the reactants passes by this adduct and reaches readily the radical species. Once the radical fragments are attained, they can recombine themselves in a second reaction to form the metal oxide structure $\text{OV}(\eta_2\text{-SO})$. In Table 2 is shown the valence electronic configuration of the lowest-lying quadruplet and doublet states of the radical fragments that differ only in the spin of the unpaired parallel electrons located on the nonmetallic fragment. As these asymptotes are degenerated, the rebounding of the radical moieties can occur along both multiplicity channels (the low-multiplicity pathway is activated when the spin of the unpaired electrons in the SO

FIGURE 1: CASSCF-MRMP2 energy profile for the V + SO₂ interaction.TABLE 1: Geometrical parameters (degrees and Å) at the stationary points located for the metal oxide OV(η_2 -SO) and the sulfide oxide SVO₂ compounds.

Structure	State	Angle		Bond distance		
		O-M-S	O-M-O	M-O	M-O	M-S
OV(η_2 -SO)	⁴ A	41.8	154.9	1.58	2.08	2.39
SVO ₂	⁴ A	112.0	136.0	1.59	1.59	2.21
OV(η_2 -SO)	² A	48.4	160.0	1.58	1.80	2.22
SVO ₂	² A	112.0	112.9	1.59	1.59	2.22
ONb(η_2 -SO)	⁴ A	38.6	113.8	1.70	2.08	2.55
SNbO ₂	⁴ A	126.5	116.7	1.92	1.71	2.39
ONb(η_2 -SO)	² A	46.2	109.4	1.71	1.88	2.37
SNbO ₂	² A	110.1	109.0	1.72	1.72	2.39
OTa(η_2 -SO)	⁴ A	36.2	131.8	1.73	2.06	2.73
STaO ₂	⁴ A	128.8	115.3	1.73	1.92	2.40
OTa(η_2 -SO)	² A	46.4	111.0	1.72	1.9	2.36
STaO ₂	² A	106.2	108.4	1.74	1.74	2.37

TABLE 2: Outermost valence configurations for the quadruplet and doublet electronic states of the radical fragments SO + MO.

Coefficient	Occupation					
VO + SO						
⁴ A	↓↑	↑	↑	↓	↑	↑
² A	↓↑	↓	↓	↓	↑	↑
	(p _x) _O	(p _z) _S	(p _x) _S	(s+p _x) _V	(d _z ²) _V	(d _{yz}) _V
NbO + SO						
⁴ A	↑	↑	↑	↑	↓	—
² A	↓	↓	↑	↑	↓	—
	(p _x) _S	(p _z) _S	(s) _{Nb}	(d _z ²) _{Nb}	(d _{yz}) _{Nb}	—
TaO + SO						
⁴ A	↑↓	↑	↑	↑	—	—
² A	↑↓	↓	↓	↑	—	—
	(s) _{Ta}	(p _z) _S	(p _y) _S	(d _z ²) _{Ta}	—	—

moiety is opposite to that corresponding to the quadruplet electronic state). The potential energy curves for the recombination of the radical fragments are shown in Figure 2.

Stable structures for the oxide complex OV(η_2 -SO) are obtained from the radical rebounding along both spin channels. The doublet electronic state is more stable than the quadruplet by 17.5 kcal/mol. As it is seen in Figure 1, the reaction along the low-multiplicity channel can evolve to the sulfide oxide SVO₂ after surmounting a relatively small energy barrier of 23.3 kcal/mol.

The potential well calculated for this product is 121.1 kcal/mol below the ground state reference and represents the global energy minimum for this interaction. For the quadruplet channel, the height of the barrier separating the OV(η_2 -SO) and the SVO₂ species is 34.3 kcal/mol; it is unlikely that the sulfide oxide could be reached along this channel under cryogenic conditions. Thus, the reaction should stop once the quadruplet complex OV(η_2 -SO) is formed.

According to the proposed scheme, the products observed under confinement conditions for this reaction are obtained from different spin-multiplicity channels. The sulfide oxide SVO₂ emerges from the rebounding reaction along the doublet channel, whereas the complex OV(η_2 -SO) is obtained when the reaction takes place through the quadruplet pathway.

3.2. Nb + SO₂ and Ta + SO₂ Reactions. In Figure 3, it is shown the two-step reaction scheme connecting the reactants with the sulfide oxide SNbO₂. This is the only product observed for this reaction. The sextuplet sulfide oxide is predicted as unstable; it lies 69.9 kcal/mol above the ground state reference. For this reason, channels emerging from the sextuplet ground state of the reactants were not investigated. However, the lowest-lying quadruplet excited state of the reactants is located 5.7 kcal/mol above the ground state

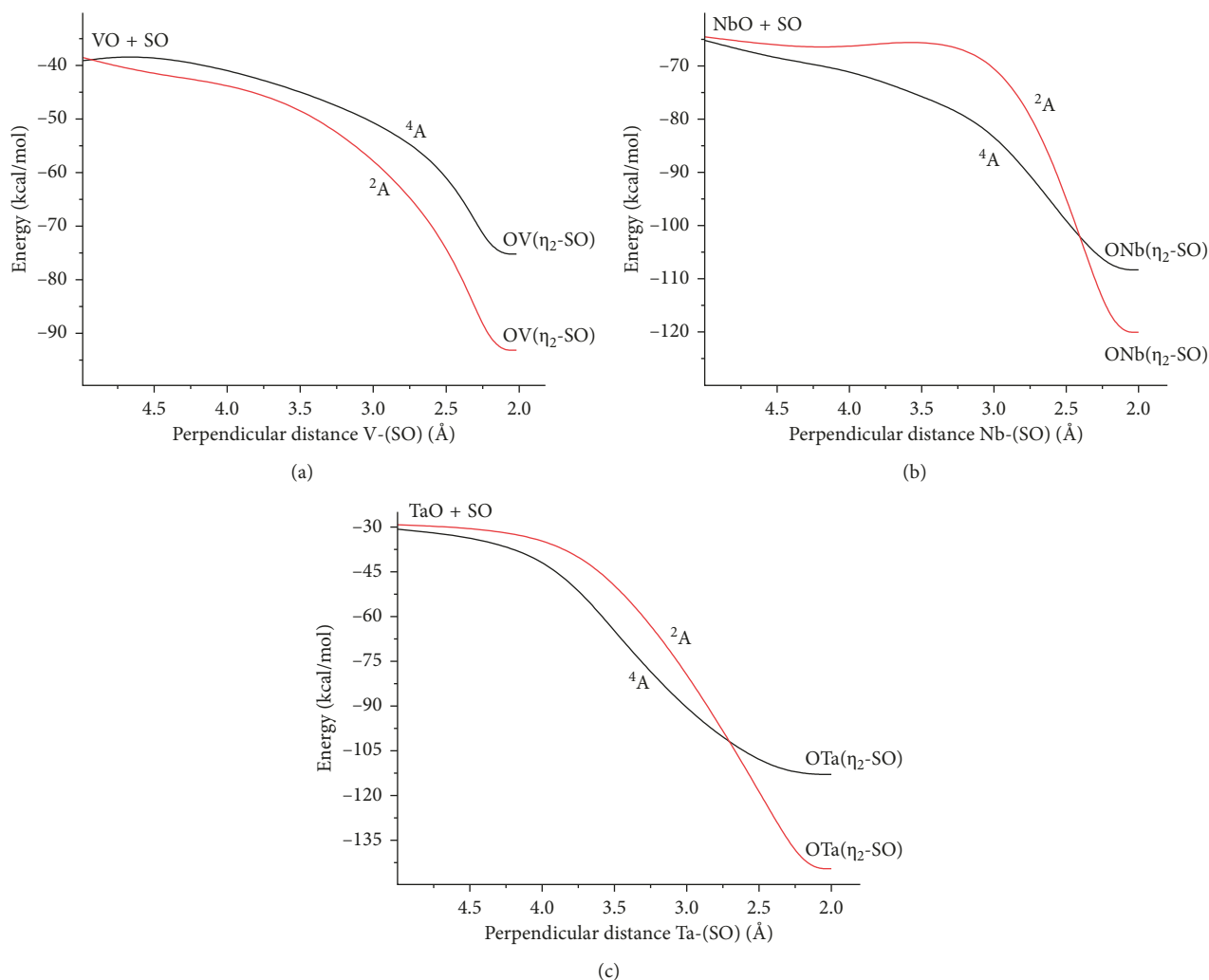


FIGURE 2: Energy plots for the recombination of the radical fragments MO + SO through the quadruplet and doublet electronic states.

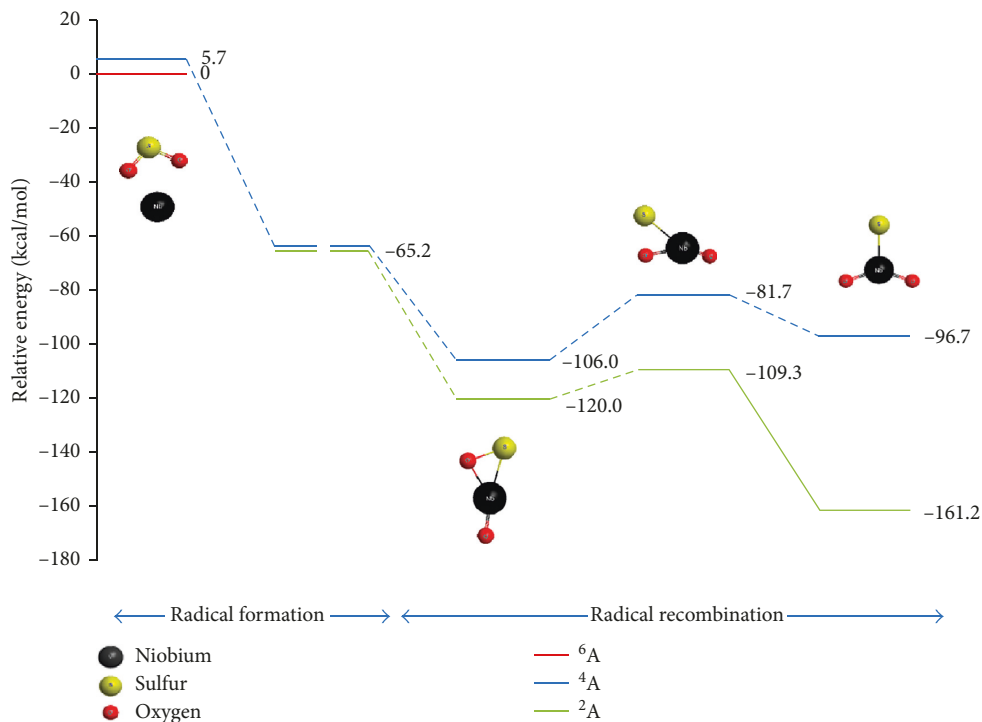
reference. It is plausible that the reaction taking place from this excited state plays an important role in determining the product distribution observed for this reaction by leading to the radical fragments NbO + SO, which lie 65.2 kcal/mol below the ground state reference.

As it is shown in Figure 3 and Table 2, the quadruplet and doublet radical asymptotes that vary only in the spin of the unpaired electrons located on the nonmetallic fragment (both parallel or antiparallel) are degenerated (-65.2 kcal/mol). Hence, recombination of the radical fragments can take place along both channels (Figure 2). The most stable structure for the complex ONb(η_2 -SO) is reached through the low-multiplicity channel. The energy minimum for this structure is located 120 kcal/mol below the ground state reference. The quadruplet state is roughly 14 kcal/mol above the doublet one. Unlike the vanadium interaction discussed before, reaction along both channels can reach the sulfide oxide SNbO₂ after surmounting in each case a relatively small energy barrier (24.3 and 10.7 kcal/mol, resp.). The doublet pathway evolves by far to the most stable sulfide oxide structure. It lies 161.2 kcal/mol below the ground state of the original reactants Nb + SO₂. Thus,

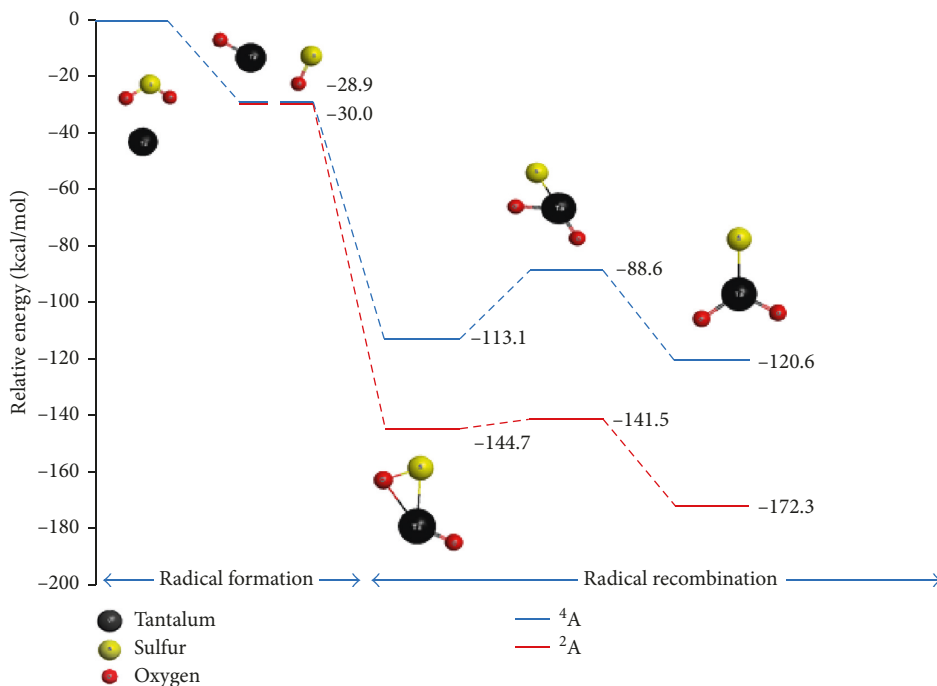
the picture attained through the two-step reaction scheme is consistent with the experimental determinations made on this interaction under cryogenic conditions, as the sulfide oxide is the only detected product.

The two-reaction scheme shown in Figure 3 for the Ta + SO₂ interaction is similar to that discussed before for the niobium reaction.

The degenerated quadruplet and doublet radical asymptotes TaO + SO are located around 30 kcal/mol below the ground state of the reactants (the small difference between the energies calculated for these asymptotes arises as consequence of the limited spaces used for the CASSCF expansions). The recombination of the radical fragments through both multiplicity channels leads to stable structures for the complex OTa(η_2 -SO). The energy potential well for the doublet state lies 144.7 kcal/mol below the ground state reference. Reaction proceeding along both the quadruplet and doublet channels could reach the sulfide oxide STaO₂ (the height of the barriers separating the OTa(η_2 -SO) and the STaO₂ species are 24.5 and 3.2 kcal/mol). As for the niobium reaction, this is the only detected product for this interaction under matrix-isolation conditions.



(a)



(b)

FIGURE 3: Energy profiles for the Nb + SO₂ and Ta + SO₂ interactions.

3.3. *Spin-Flip Models versus the Two-Step Reaction Scheme.* The picture attained for the investigated interactions in terms of two sequential reactions involving the radical fragments OM + SO is consistent with the product distribution determined for them in the IR-matrix spectra [17]. This scheme provides a plausible explanation for the

low-spin products determined for these reactions without invoking unlikely interactions between electronic states of different spin multiplicity, as it has been proposed in the previous study by Liu et al. [17]. This could be of significance for the interactions of vanadium and niobium, as it is not expected that spin-orbit effects would be relevant in the

description of their energy profiles. However, it is important stressing out that the corresponding reaction with tantalum is also suitably described by this model.

According to the proposed scheme, the recombination of the radical fragments through the low-multiplicity channel leads in all the cases to the products observed under matrix-isolation conditions. As the radical species formed in the first reaction would remain trapped, presumably the confinement imposed by the matrix could play an important role in determining the observed product distributions by enabling their recombination.

In a previous contribution, the results obtained from matrix-isolation determinations for the reactions of V, Nb, and Ta with CH_3CN were described in terms of a similar reaction scheme involving the radical species $\text{CH}_3 + \text{MNC}$ [19]. As for the reactions with SO_2 discussed here, the products determined for those reactions evolve from the doublet channel activated by the rebounding of radical fragments with opposite spin. It is striking that the same scheme explains for the main features determined for these groups of reactions.

Interestingly, the product distributions obtained under confinement conditions for other reactions have been analyzed by using a similar reaction scheme. The low-spin carbenes and carbynes detected in the IR-matrix spectra for the reactions of zirconium, iron, and ruthenium with fluoromethanes were rationalized by means of two sequential radical reactions [26–28]. Likewise, in a recent contribution, we have extended the use of this scheme to the description of interactions involving transition-metal complexes. Particularly, we used this model to rationalize the irregularities observed in the product distribution determined for the reactions of triethyl-methane and silane molecules with the CpCoCo and CpCORh compounds [29]. Unlike previous studies on these interactions, in the above-mentioned investigations, we have not invoked interactions between the potential energy surfaces belonging to electronic states of different spin-multiplicity to explain for the low-spin species observed for these reactions [30–35]. Hence, the use of this sequential radical reaction scheme overcomes the main disadvantage of the spin-flip models [36–38]. The relativistic effects that could lead to interactions between electronic states of different spin multiplicity can be relevant in reactions involving heavy atoms, but not in those in which only lighter atoms participate.

In fact, important mechanistic aspects can be missed or hidden when spin-flip models are applied to reactions involving only light atoms. As discussed before, the product distribution detected for the reaction of vanadium with SO_2 is different from those observed for the corresponding reactions with niobium and tantalum. Whereas for the vanadium reaction are detected both the oxide $\text{OV}(\eta_2\text{-SO})$ and the sulfide oxide SVO_2 complexes, for the remaining reactions only the sulfide oxide is yielded [17]. According to the proposed scheme, the products observed for the vanadium interaction evolve from different spin channels. Reaction along the doublet channel reaches readily the sulfide oxide complex SVO_2 . However, due to the high energy barrier separating the $\text{OV}(\eta_2\text{-SO})$ and the SVO_2 compounds

(34.2 kcal/mol), it is expected that the reaction through the quadruplet pathway ends when the oxide $\text{OV}(\eta_2\text{-SO})$ is yielded. For the corresponding reactions with niobium and tantalum, the height of the energy barriers for the high-multiplicity channels is lower (around 24 kcal/mol in each case). For these interactions, both the quadruplet and doublet channels could attain the sulfide oxide. This interpretation is essentially different from that given by Liu et al. [17]. These authors explain the differences in the product distributions observed for these interactions in terms of the relative stability of the doublet $\text{OM}(\eta_2\text{-SO})$ and the SMO_2 complexes (the role played by the quadruplet state is missed once the intersystem crossing occurs).

4. Conclusions

The reactions of the SO_2 molecule with the V, Nb, and Ta atoms have been studied theoretically through DFT and CASSCF-MRMP2 calculations. Energy profiles joining the ground state of the reactants with the products observed under cryogenic matrix-isolation conditions have been built for the three interactions by using a two-step reaction scheme involving the radical species $\text{MO} + \text{SO}$.

The description attained for each of the investigated interactions allows explaining for the low-spin products observed for them in the IR-matrix spectra without invoking interactions between electronic states of different spin multiplicity, as it has been proposed in a previous study. The use of this model also allows highlighting subtle aspects that can play an important role in determining the product distributions for these interactions.

Conflicts of Interest

The authors declare that they have no conflicts of interest.

Acknowledgments

This research was supported by the Universidad Nacional Autónoma de México (DGAPA-IN113515). The authors acknowledge the computational resources provided by DGCTIC-UNAM for the use of the Miztli supercomputer. C. Velásquez gratefully acknowledges CONACYT for his graduate scholarship (576688). A. E. Torres gratefully acknowledges CONACYT for the postdoctoral scholarship (364788/245467).

References

- [1] E. Robinson and R. Robbins, "Gaseous sulfur pollutants from urban and natural sources," *Journal of the Air Pollution Control Association*, vol. 20, no. 4, pp. 233–235, 1970.
- [2] Y. Sun, E. Zwolińska, and A. G. Chmielewski, "Abatement technologies for high concentrations of NO_x and SO_2 removal from exhaust gases: a review," *Critical Reviews in Environmental Science and Technology*, vol. 46, no. 2, pp. 119–142, 2016.
- [3] P. G. Menon, "Diagnosis of industrial catalyst deactivation by surface characterization techniques," *Chemical Reviews*, vol. 94, no. 4, pp. 1021–1046, 1994.
- [4] S. Matsumoto, "Recent advances in automobile exhaust catalysts," *Catalysis Today*, vol. 90, no. 3–4, pp. 183–190, 2004.

- [5] J. A. Rodriguez, T. Jirsak, S. Chaturvedi, and J. Hrbek, "Surface chemistry of SO₂ on Sn and Sn/Pt(111) Alloys: effects of metal-metal bonding on reactivity toward sulfur," *Journal of the American Chemical Society*, vol. 120, no. 43, pp. 11149–11157, 1998.
- [6] S. Chaturvedi, J. A. Rodriguez, T. Jirsak, and J. Hrbek, "Surface chemistry of SO₂ on Zn and ZnO: photoemission and molecular orbital studies," *Journal of Physical Chemistry B*, vol. 102, no. 36, pp. 7033–7043, 1998.
- [7] N. Luckas, K. Gotterbarm, R. Streber et al., "Adsorption and reaction of SO₂ on clean and oxygen precovered Pd(100)—a combined HR-XPS and DF study," *Physical Chemistry Chemical Physics*, vol. 13, no. 36, p. 16227, 2011.
- [8] J. A. Rodriguez, T. Jirsak, A. Freitag, J. Larese, and A. Maiti, "Interaction of SO₂ with MgO(100) and Cu/MgO(100): decomposition reactions and the formation of SO₃ and SO₄," *Journal of Physical Chemistry B*, vol. 104, no. 31, pp. 7439–7448, 2000.
- [9] M. Happel, N. Luckas, F. Vines, M. Sobota, M. Laurin, and J. Libuda, "SO₂ adsorption on Pt(111) and oxygen precovered Pt(111): a combined infrared reflection absorption spectroscopy and density functional study," *Journal of Physical Chemistry C*, vol. 115, no. 2, pp. 479–491, 2011.
- [10] R. E. McClean, M. L. Campbell, and E. J. Kolsch, "Depletion kinetics of niobium atoms in the gas phase," *Journal of Physical Chemistry A*, vol. 101, no. 18, pp. 3348–3355, 1997.
- [11] M. L. Campbell and R. E. McClean, "Kinetics of neutral transition-metal atoms in the gas phase: oxidation reactions of titanium (a3F) from 300 to 600 K," *Journal of Physical Chemistry*, vol. 97, no. 30, pp. 7942–7946, 1993.
- [12] M. L. Campbell, K. L. Hooper, and E. J. Kolsch, "Temperature dependent study of the kinetics of Sc(a2D3/2) with O₂, N₂O, CO₂, NO and SO₂," *Chemical Physics Letters*, vol. 274, no. 1–3, pp. 7–12, 1997.
- [13] R. E. McClean, "Depletion kinetics of chromium atoms by sulfur dioxide," *Journal of Physical Chemistry A*, vol. 104, no. 38, pp. 8723–8729, 2000.
- [14] R. E. McClean and L. Norris, "A kinetic study of the reactions of vanadium, iron, and cobalt with sulfur dioxide," *Physical Chemistry Chemical Physics*, vol. 7, no. 12, p. 2489, 2005.
- [15] X. Liu, X. F. Wang, Q. Wang, and L. Andrews, "OMS, OM(η²-SO), and OM(η²-SO)(η²-SO₂) molecules (M = Ti, Zr, Hf): infrared spectra and density functional calculations," *Inorganic Chemistry*, vol. 51, no. 13, pp. 7415–7424, 2012.
- [16] X. F. Wang and L. Andrews, "Infrared spectra and density functional calculations for SMO₂ molecules (M = Cr, Mo, W)," *Journal of Physical Chemistry A*, vol. 113, no. 31, pp. 8934–8941, 2009.
- [17] X. Liu, X. Wang, Q. Wang, and L. Andrews, "Spontaneous sulfur dioxide activation by Group V metal (V, Nb, Ta) atoms in excess argon at cryogenic temperatures," *Physical Chemistry Chemical Physics*, vol. 15, no. 24, p. 9823, 2013.
- [18] J. E. Sansonetti and W. C. Martin, "Handbook of basic atomic spectroscopic data," *Journal of Physical and Chemical Reference Data*, vol. 34, no. 4, pp. 1559–2259, 2005.
- [19] I. Flores, A. E. Torres, and F. Colmenares, "Rationalizing the low-spin products observed for the reactions M+CH₃ CN (M=V, Nb, Ta) through a non-spin flip scheme," *ChemistrySelect*, vol. 2, no. 11, pp. 3216–3222, 2017.
- [20] F. Weigend and R. Ahlrichs, "Balanced basis sets of split valence, triple zeta valence and quadruple zeta valence quality for H to Rn: design and assessment of accuracy," *Physical Chemistry Chemical Physics*, vol. 7, no. 18, p. 3297, 2005.
- [21] K. L. Schuchardt, B. T. Didier, T. Elsethagen et al., "Basis set exchange: a community database for computational sciences," *Journal of Chemical Information and Modeling*, vol. 47, no. 3, pp. 1045–1052, 2007.
- [22] D. Feller, "The role of databases in support of computational chemistry calculations," *Journal of Computational Chemistry*, vol. 17, no. 13, pp. 1571–1586, 1996.
- [23] D. Andrae, U. Haussermann, M. Dolg, H. Stoll, and H. Preuss, "Energy-adjusted ab initio pseudopotentials for the second and third row transition elements," *Theoretica Chimica Acta*, vol. 77, no. 2, pp. 123–141, 1990.
- [24] M. W. Schmidt, K. K. Baldrige, J. A. Boatz et al., "General atomic and molecular electronic structure system," *Journal of Computational Chemistry*, vol. 14, no. 11, pp. 1347–1363, 1993.
- [25] M. J. Frisch, G. W. Trucks, H. B. Schlegel et al., *Gaussian 09, Revision A.02*, Gaussian Inc., Wallingford, CT, USA, 2016.
- [26] A. E. Torres, G. Castro, R. Pablo-Pedro, and F. Colmenares, "A two-step reaction scheme leading to singlet carbene species that can be detected under matrix conditions for the reaction of Zr(3F) with either CH₃F or CH₃CN," *Journal of Computational Chemistry*, vol. 35, no. 11, pp. 883–890, 2014.
- [27] A. E. Torres, O. Méndez, and F. Colmenares, "Two-step radical reactions that switch low multiplicity channels leading to the carbene and carbyne species detected for Ru(⁵F) + CH_{4-n}F_n (n = 2–4) interactions under matrix isolation conditions," *RSC Advances*, vol. 3, no. 29, pp. 11607–11613, 2013.
- [28] G. Castro, R. Pablo-Pedro, and F. Colmenares, "Use of a two-sequential radical reaction scheme to rationalise the high-oxidation-state carbene species detected under confinement conditions for the interactions Fe(⁵D) + CH_{4-n}F_n (n = 2–4)," *Molecular Physics*, vol. 115, no. 19, pp. 2405–2410, 2017.
- [29] G. Castro and F. Colmenares, "Using a non-spin flip model to rationalize the irregular patterns observed in the activation of the C–H and Si–H bonds of small molecules by CpMCO (M = Co, Rh) complexes," *Physical Chemistry Chemical Physics*, vol. 19, no. 36, pp. 25115–25121, 2017.
- [30] H.-G. Cho and L. Andrews, "Persistent photo-reversible transition-metal methyldene system generated from reaction of methyl fluoride with laser-ablated zirconium atoms and isolated in a solid argon matrix," *Journal of the American Chemical Society*, vol. 126, no. 33, pp. 10485–10492, 2004.
- [31] H.-G. Cho, J. T. Lyon, and L. Andrews, "Reactions of laser-ablated iron atoms with halomethanes: infrared spectra, density functional calculations, and structures of simple iron insertion and methyldene complexes," *Organometallics*, vol. 27, no. 20, pp. 5241–5251, 2008.
- [32] H. G. Cho and L. Andrews, "Infrared spectra of insertion, methyldene, and methyldyne complexes in reactions of laser-ablated ruthenium atoms with halomethanes and methane," *European Journal of Inorganic Chemistry*, vol. 16, pp. 2537–2549, 2008.
- [33] E. P. Wasserman, C. B. Moore, and R. G. Bergman, "Gas-phase rates of alkane C–H oxidative addition to a transient CpRh(CO) complex," *Science*, vol. 255, no. 5042, pp. 315–318, 1992.
- [34] J. P. Lomont, S. C. Nguyen, and C. B. Harris, "Ultrafast infrared studies of the role of spin states in organometallic reaction dynamics," *Accounts of Chemical Research*, vol. 47, no. 5, pp. 1634–1642, 2014.
- [35] P. T. Snee, C. K. Payne, K. T. Kotz, H. Yang, and C. B. Harris, "Triplet organometallic reactivity under ambient conditions: an ultrafast UV pump/IR probe study," *Journal of the American Chemical Society*, vol. 123, no. 10, pp. 2255–2264, 2001.

- [36] D. Schröder, S. Shaik, and H. Schwarz, "Two-state reactivity as a new concept in organometallic chemistry," *Accounts of Chemical Research*, vol. 33, no. 3, pp. 139–145, 2000.
- [37] P. Gütllich, Y. Garcia, and H. A. Goodwin, "Spin crossover phenomena in Fe(II) complexes," *Chemical Society Reviews*, vol. 29, no. 6, pp. 419–427, 2000.
- [38] R. Poli and J. N. Harvey, "Spin forbidden chemical reactions of transition metal compounds. New ideas and new computational challenges," *Chemical Society Reviews*, vol. 32, no. 1, pp. 1–8, 2003.

